

# 290 and 340 nm UV LED arrays for fluorescence detection from single airborne particles

Kristina Davitt, Yoon-Kyu Song, William R. Patterson III, and Arto V. Nurmikko

*Brown University, Division of Engineering, Providence, RI 02912, USA*

[Kristina\\_Davitt@brown.edu](mailto:Kristina_Davitt@brown.edu)

Maria Gherasimova and Jung Han

*Yale University, Department of Electrical Engineering, New Haven CT 06520, USA*

Yong-Le Pan and Richard K. Chang

*Yale University, Department of Applied Physics and Center from Laser Diagnostics, New Haven CT 06520, USA*

**Abstract:** We demonstrate a compact system, incorporating a 32-element linear array of ultraviolet (290 nm and 340 nm) light-emitting diodes (LEDs) and a multi-anode photomultiplier tube, to the in-flight fluorescence detection of aerosolized particles, here containing the biological molecules tryptophan and NADH. This system illustrates substantial advances in the growth and fabrication of new semiconductor UV light emitting devices and an evolution in packaging details for LEDs tailored to the bio-aerosol warning problem. Optical engineering strategies are employed which take advantage of the size and versatility of light-emitting diodes to develop a truly compact fluorescence detector.

©2005 Optical Society of America

**OCIS codes:** (120.0120) Instrumentation; (010.1100) Aerosol Detection; (230.3670) Light-emitting diodes; (170.6280) Spectroscopy, fluorescence and luminescence; (220.4840) Optical Testing

---

## References and links

1. Joseph R. Lakowicz in *Principles of Fluorescence Spectroscopy*, (Kluwer Academic / Plenum Publishers, New York, NY, 1999).
2. S.C. Hill, R.G. Pinnick, S. Niles, Y.L. Pan, S. Holler, R.K. Chang, J. Bottiger, B.T. Chen, C.S. Orr and G. Feather, "Real-Time Measurement of Fluorescence Spectra from Single Airborne Biological Particles," *Field Anal. Chem. and Tech.* **3** (4-5), 221-239 (1999).
3. V. Sivaprakasam, A.L. Huston, C. Scotto and J.D. Eversole, "Multiple UV wavelength excitation and fluorescence of bioaerosols," *Opt. Express* **12**, 19, 4457-4466 (2004).
4. P.P. Hairston, J. Ho and F.R. Quant, "Design of an instrument for real-time detection of bioaerosols using simultaneous measurement of particle aerodynamic size and intrinsic fluorescence," *J. Aerosol Sci.* **28**, 3, 471-482 (1997).
5. L.M. Brosseau, D. Vesley, N. Rice, K. Goodell, M. Nellis and P. Hairston, "Differences in Detected Fluorescence Among Several Bacterial Species Measured with a Direct-Reading Particle Sizer and Fluorescence Detector," *Aerosol Sci. and Tech.* **32**, 545-558 (2000).
6. P.H. Kaye, W.R. Stanley, E. Hirst, E.V. Foot, K.L. Baxter and S.J. Barrington, "Single particle multichannel bio-aerosol fluorescence sensor," *Opt. Express* **13**, 10, 3583-3593 (2005).
7. Y.L. Pan, J. Hartings, R.G. Pinnick, S.C. Hill, J. Halverson and R.K. Chang, "Single-Particle Fluorescence Spectrometer for Ambient Aerosols," *Aerosol Sci. and Tech.* **37**, 628-639 (2003).
8. Y.L. Pan, V. Boutou, J.R. Bottiger, S.S. Zhang, J.P. Wolf and R.K. Chang, "A Puff of Air Sorts Bioaerosols for Pathogen Identification," *Aerosol Sci. and Tech.* **38**, 598-602 (2004).
9. V. Adivarahan, S. Wu, W.H. Sun, V. Mandavilli, M.S. Shatalov, G. Simin, J.W. Yang, H.P. Maruska and M.A. Khan, "High-power deep ultraviolet light-emitting diodes based on a micro-pixel design," *Appl. Phys. Lett.* **85**, 10, 1838-1840, (2004).
10. S.R. Jeon, M. Gherasimova, Z. Ren, J. Su, G. Cui, J. Han, H. Peng, Y.K. Song, A.V. Nurmikko, L. Zhou, W. Goetz and M. Krames. "High Performance AlGaInN Ultraviolet Light-Emitting Diode at the 340nm Wavelength," *Jpn. J. Appl. Phys.* **43**, 11A, L1409-1412 (2004).
11. Y.L. Pan, V. Boutou, R.K. Chang, I. Ozden, K. Davitt and A.V. Nurmikko, "Application of light-emitting diodes for fluorescence detection," *Opt. Lett.* **28**, 18, 1707-1709 (2003).

12. Jesse Mohn, Department of Applied Physics, Yale University (unpublished results, 2003).
  13. S.C. Hill, R.G. Pinnick, S. Niles, N.F. Fell Jr., Y.L. Pan, J. Bottiger, B.V. Bronk, S. Holler and R.K. Chang, "Fluorescence from airborne microparticles: dependence on size, concentration of fluorophores, and illumination intensity," *Appl. Opt.* **40**, 18, 3005-3013 (2001).
  14. Y.L. Pan, P. Cobler, S. Rhodes, A. Potter, T. Chou, S. Holler, R.K. Chang, R.G. Pinnick, J.P. Wolf, "High-speed, high-sensitivity aerosol fluorescence spectrum detection using a 32-anode photomultiplier tube detector," *Rev. Sci. Instrum.* **72**, 3, 1831-1836 (2001); VTech Engineering, Andover MA
  15. J.R. Bottiger and P.J. DeLuca, "Low Concentration Aerosol Generator," United States Patent No. 5,918,254 (1999).
- 

## 1. Introduction

Ultraviolet laser-induced fluorescence (UV-LIF) is a standard technique used to discriminate between aerosolized particles; however, the large system size and cost hinders widespread use of this technique in the field. Emerging semiconductor UV sources permit miniaturization and cost reduction of these and other systems previously employing traditional UV solid-state lasers.

Typically, biological materials contain key constituent molecules such as the amino acids tryptophan and tyrosine, and reduced nicotinamide adenine dinucleotide (NADH) which exhibit considerable absorption only below 300 nm, with the exception of NADH which has a local absorption maximum at 340 nm. These compounds exhibit characteristic fluorescence emission spectra [1], enabling discrimination between particles of biological origin and non-biological origin, and possibly between species of the former. Fluorescence studies on bacterial spores show fluorescence peaks attributed to tryptophan and NADH in particular, hence the target LIF excitation wavelengths of 280 nm and 340 nm respectively [2]. (Here we attribute the broad 450 nm emission seen in preparations of bacterial spores to NADH, although there remains some debate about the origin of this fluorescence [3].) Robust semiconductor lasers operating at 340 nm and below do not exist today, however, light emitting diodes (LEDs) are emerging in this wavelength range. State of the art InGaN-based sources in the 370-380 nm range lie on the edge of the NADH absorption spectrum and as such, despite presently higher quantum efficiencies, are much less useful than the more challenging quaternary AlGaInN-based 340 nm devices and, especially, the ternary AlGaInN-based 270-290 nm devices.

Aerosol UV-LIF detection systems may be broadly characterized as either those that employ an integrated fluorescence intensity measurement [4-6] using spectral filters to isolate the tryptophan and NADH fluorescence bands, or those that use a spectrometer for more complete spectral data acquisition [7]. Here we demonstrate the versatility of new UV LEDs as UV sources in both the spectral filter-based and spectrometer-based compact aerosol fluorescence detection systems using linear arrays of 340 nm and 290 nm emitters. In keeping with the aim of miniaturizing the entire system, for the latter case we integrated the active optics with a compact spectrometer, including a multi-anode photomultiplier (PMT), for acquiring 32-point spectra.

The spatial incoherence of an LED source requires adaptation in the optical system design for delivery of a maximum possible excitation flux to the moving aerosol particle target. On the other hand, LEDs offer the advantage that the device geometry, and hence illumination pattern, can be easily tailored to accommodate a specific task. In the application demonstration described below, airborne fluorophores are vertically ejected from a nozzle and the individual elements of the UV LED array are fired in rapid sequence so as to track a particle and continuously illuminate it during its time-of-flight. A linear array of separate UV LEDs offers several advantages over a single element device; an increase in the total energy delivered to the particle, which is achieved both by extending the excitation time as well as enabling the use of higher injection currents, and a reduction in the background signal. We note that our UV LED array-based spectroscopic single particle in-flight fluorescence has

broader potential as an analytical tool in applications of “multiwell” based approaches to biochemical assaying.

## 2. Device design

In an LED-IF apparatus, as in standard LIF systems for aerosol analysis, particles are collected from the ambient air and ejected through a nozzle into the optical cell. In a standalone system, particle collection is usually accomplished with a virtual-impactor particle concentrator. In this demonstration particles are not random or from the ambient, rather we generate known particles for the purposes of testing the system response. For the particular nozzle used in this demonstration, the particle flow remains laminar for at least 1 cm, and the width of the jet stream is approximately 200  $\mu\text{m}$ . These dimensions are met by our design and fabrication of a 32-element linear array of UV LEDs composed of individual elements 200  $\mu\text{m}$  wide and 50  $\mu\text{m}$  high, illustrated in Fig.1. In order to accommodate the n-electrodes, the center-to-center separation of adjacent LEDs is 100  $\mu\text{m}$ , yielding a total array height of approximately 3.2 mm. The LED width ensures that most particles emerging from the nozzle are illuminated throughout their trajectory; the total array height of 3.2 mm enables it to fit comfortably within the stable jet stream while allowing for further components such as “triggering optics” employing elastic scattering above the fluorescence zone and an aerodynamic deflector following this zone [8]. Each of the 32-elements of the array is individually addressable while sharing a common n-electrode. The finger-like design of the n-contact between each optical aperture ensures that the lateral n to p distance in these mesa-etched devices is never more than 20  $\mu\text{m}$ , mitigating current-crowding effects that challenged early material growths, and which are one important device issue in emerging sub-300 nm semiconductor emitters [9].

The 290 nm and 340 nm LEDs were fabricated from MOCVD-grown AlGaIn and AlGaInN, quantum-well p-n junction heterostructures respectively [10], grown epitaxially on sapphire substrates. In contrast to an early demonstration of the possible utility of InGaIn blue LED arrays [11], in which top-side emission of blue LEDs equipped with individual microlenses was extracted through a semi-transparent p-electrode, the new UV LED arrays employ a different light extraction strategy. In particular, the emission from the UV LEDs is now extracted through the transparent sapphire backside. An opaque Ni/Au p-contact was employed, and the array was flip-chipped onto a patterned silicon submount for electrical contact and thermal management using electrically and thermally conductive epoxies respectively. A single hyperhemispherical sapphire lens spanning over the entire array was fixed to the polished backside with  $n = 1.56$  UV-transparent epoxy. Ray-tracing simulations indicate that the inclusion of the integrated sapphire lens improves the transfer efficiency of light from the array to the 200  $\mu\text{m}$  wide particle trajectory by a factor of 3 [12]. This improvement, which has been experimentally verified, arises from both an improved light extraction efficiency as well as serving as the first stage in the collection optics. More valuable than improvements to the array geometry to match the particle jetstream or advances in packaging and light extraction from the LEDs, the reduction in wavelength from 460 nm in [11] to 340 nm and 290 nm represents a significant advance in the field of semiconductor light emitters and enables an LED-based system to target bio-fluorophores present in bacterial spores and hence offer a viable alternative to current laser-based aerosol detection systems.

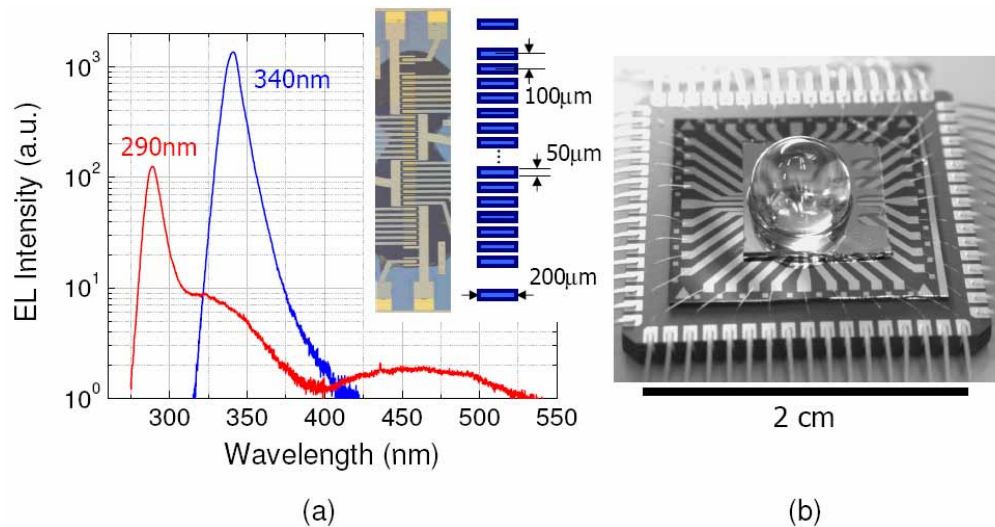


Fig. 1. (a) Electroluminescence spectra on a semi-log scale taken under  $1 \text{ kA/cm}^2$  injection current from typical elements of a 290 nm and 340 nm linear array. Light output axes scaled and not comparable for different devices. Inset shows array geometry and individual LED element dimensions. (b) Photographic image of packaged array.

Unpackaged 340 nm wavelength LEDs capable of producing 1 mW CW output power per element at a current injection of  $1 \text{ kA/cm}^2$  have been achieved in array fabrications. Similar arrays of 290 nm devices yield CW output powers of 100  $\mu\text{W}$  per element. A long-wavelength tail, as shown in the electroluminescence spectra of Fig.1(a) (semi-log scale), is a potential problem for a bio-aerosol detection system as it can overlap significantly with the fluorescence bands of interest, particularly in the case of a sub-300 nm UV LED targeting tryptophan. In the case of the 290 nm LED, at a current injection of  $1 \text{ kA/cm}^2$ , approximately 30% of the light output power is at wavelengths longer than 310 nm. Owing to the narrow separation between fluorescence excitation (290 nm/340 nm) and emission (310-400 nm / 400-550 nm) and the weak fluorescence signal, a judicious choice of excitation filters is required.

### 3. System design and experimental results

In our testbed, airborne particles were generated with a piezo-electric generator (MicroDrop GmbH). Initial tests were performed using nominally 70  $\mu\text{m}$  diameter water droplets, selectively doped with either NADH or tryptophan, depending on the LED wavelength under test. Droplets were produced on demand by a trigger to the piezo-electric generator, and a trigger and timing circuit controlled the delay between particle generation and the firing of the first element of the array, as well as the clock determining the sequential LED firing rate in order to synchronize with the particle velocity of approximately 2 m/sec. Since a single water droplet with fixed delay is created from each trigger to the generator, the subsequent timing is tied to this trigger and there is no initial need for the elastic scatter trigger channel introduced later in this demonstration.

In both the optical filter-based and spectroscopic systems, we used a narrow bandpass filter to block the well-known long-wavelength tail associated with the LED. In the 340 nm LED case, an excitation filter centered at 330nm with a 50% transmission-maximum bandwidth of 75nm, rejects unwanted LED emission to better than OD4.5 in the NADH fluorescence band; under 290 nm UV LED excitation the filter is centered at 275nm with a bandwidth of 50nm and blocks better than OD3 in the tryptophan band. After the filter, a pair of short focal length, high NA ( $f = 16\text{mm}$ ,  $F\# 1.3$ ), sapphire plano-convex lenses imaged the 32-element UV LED array onto the particle jet stream with a magnification of 1. Thus, the

sequential firing of elements of the LED array results in a spatial tracking of the particle during approximately 3.2mm of its trajectory. The geometry of light collection is limited due to the large LED background, hence the collection optics are located at right angles to the incident beam.

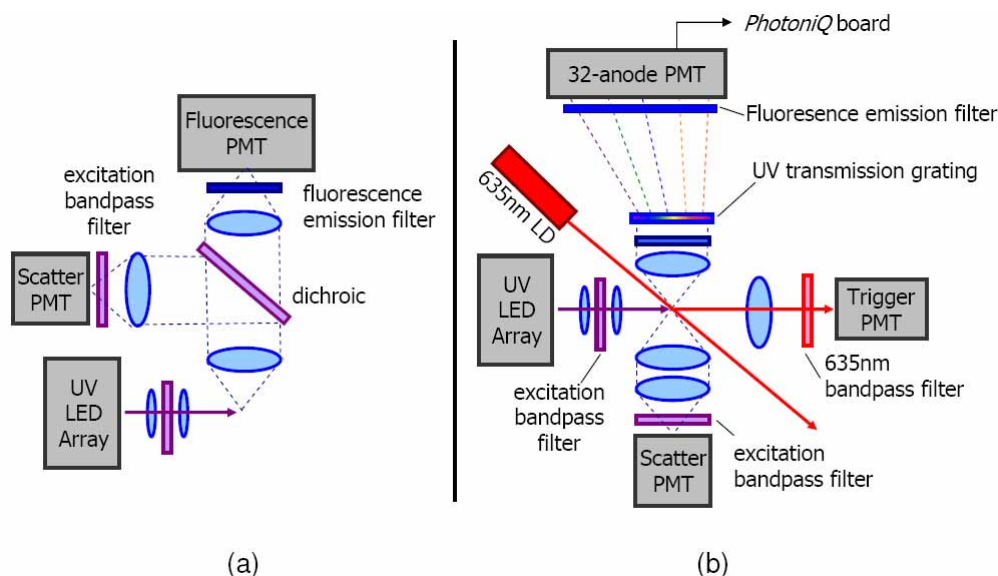


Fig. 2. Top-view schematics of two compact LED array-based detection systems. (a) Optical filter-based and (b) spectroscopic fluorescence detection.

### 3.1 Optical filter-based detection

The optical system shown in Fig. 2(a) consisted of a spectral-filter based detection scheme and occupied a footprint of approximately 20 cm x 13 cm. As an example, we present here an application demonstration of a 340 nm LED array targeting NADH, in which case a dichroic filter was used to separate and redirect the scatter and fluorescence signals. Two PMTs, with additional individual filters to isolate the 340 nm scatter and 400-550 nm NADH fluorescence, captured single-particle data, such as the traces in Fig.3(a). The filter for the scatter channel is a duplicate of the excitation filter, and the fluorescence emission filter is a long-pass filter with a 50% transmission point at 390nm. In this case, each element of the LED array is pulsed for 70  $\mu$ sec with a bias of 40 mA, yielding an output power of approximately 1 mW immediately following the hyperhemispherical lens. Simultaneously recorded scattering data serve as a means to normalize the fluorescence data by removing particle size dependences and correcting for possible deviations of a particle from the illumination volume during its trajectory. Total fluorescence and scattering signals are obtained by integrating the data over the approximately 2.5 msec of illumination time. As a means to characterize the system response, a ratio of the total fluorescence and scattering signals (F/S) was determined as a function of NADH concentration in similarly sized doped water droplets; shown in Fig.3(b) (open circles). The indicated background NADH signal reflects the signal measured from undoped water droplets and represents leakage of light into the fluorescence channel. In this spectral-filter based scheme, NADH concentrations of 0.01% by weight (140  $\mu$ Molar) are readily detectable with a modestly performing array.

A similar filter-based system now operating with a 290nm LED array to target tryptophan fluorescence has also been tested. In this case the fluorescence emission is collected through a 305 nm long-pass filter. Under the same pulse conditions, each element of the array is

operated with a bias of 20 mA, yielding an output power of approximately 45  $\mu$ W. Figure 3(b) (closed circles) shows the F/S characterization of this system. We note that the fluorescence increases sublinearly with tryptophan concentration above 0.1%, an effect which has been observed by others [13], and which may be attributed to self-quenching as the concentration approaches the solubility limit of tryptophan in water. The spectral-filter based 290nm array scheme is capable of detecting tryptophan concentrations below 0.0025% (125  $\mu$ Molar).

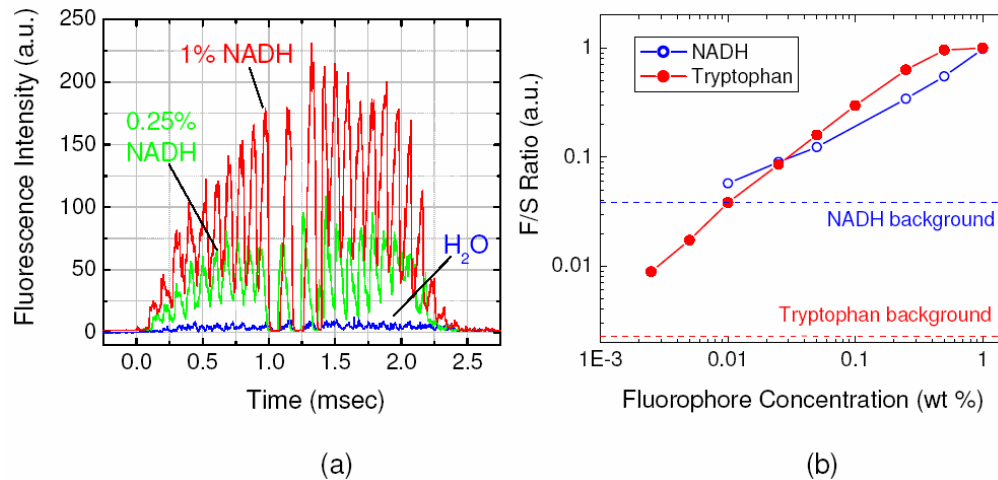


Fig. 3. Optical filter-based system response to fluorophore-doped water droplets. (a) Real-time fluorescence channel recordings for single NADH particles (with two non-functioning 340nm LED array elements after the 1 msec mark) shown for two concentration levels measured against pure H<sub>2</sub>O, and (b) the measured fluorescence to scatter ratios for both the 290nm array targeting tryptophan (closed circles) and the 340nm array targeting NADH (open circles).

### 3.2 Spectroscopic detection

Figure 2(b) illustrates the optical setup for a 32-point, particle in-flight, spectroscopic fluorescence detection strategy. The array and imaging optics are identical to the filter-based scheme, however, the system has a slightly larger footprint of approximately 25 x 35 cm. Also, in this case a 635 nm laser diode (LD) was focused to the jet stream immediately emerging from the nozzle, and an associated PMT with a red bandpass filter (630nm center, 40nm bandwidth) served as a trigger to indicate the presence of a particle in the system and cue the timing electronics. This feature anticipated the use of the system with dry particles sampled from the ambient which, unlike the water droplets which were generated on demand by the piezo-electric generator and thus required no additional indication of their presence in the system, are not artificially generated and arrive at random times.

Scatter at the LED wavelength is collected by a pair of plano-convex lenses and a simple PMT. The fluorescence channel consists of a collection lens, an LED-scatter blocking filter and a fluorescence emission filter; a UV transmission grating is used to spectrally disperse the light onto a 32-anode PMT. Placed directly in front of the PMT, the fluorescence emission filter is used to block scattered 635 nm light from the LD and scattered LED light (at either 340 nm or 290 nm) while passing the fluorophore fluorescence band. In the case of the 340 nm LED, the same filters described above were used, however, in the case of the 290 nm LED, a single commercial filter with this capability could not be found, and an additional LED-scatter blocking filter is required. We used a piece of filter glass (360 nm center, 160 nm bandwidth) to block the LD light, followed by a 305 nm longpass filter to block the LED scatter. We have found that the choice of a transmission grating offers greater flexibility in

geometry than a concave holographic grating, in part due to the large background LED emission. The multi-anode PMT was controlled by an electronics interface card (PhotoniQ board from Vtech Engineering Corp.) [14], such that fluorescence spectra were collected with an integration time of 2.5 msec, which is equal to the total illumination time of each particle. The combination of a transmission grating and multi-anode PMT for the detector portion of the system is in keeping with the reduction in size and cost offered by the use of LEDs as UV sources. Compared to both traditional spectral detection systems using CCDs and to the initial demonstration of a multi-anode PMT for rapid spectrum collection [14], which still employed a large spectrograph and solid-state laser, this represents a step towards a truly miniaturized instrument with comparable function. Figure 4(a) shows 10 single particle fluorescence spectra collected from 10 successive particles of 0.025% NADH illuminated by a sequentially firing 340 nm UV LED array. To improve the spectral shape for the purpose of allowing for further discrimination routines to analyze a spectrum, a simple 3-point adjacent-average,  $x'(n) = \frac{1}{3}[x(n-1) + x(n) + x(n+1)]$ , is performed on the 32-point spectral data from each particle. This routine maintains the single-particle nature of the spectrum; that is, it does not time-average over sequential particles to improve the signal-to-noise. Thus, the implementation of this algorithm still permits real-time processing of particles such as with an aerodynamic deflector. Thus, with a modestly performing 340 nm LED array, the spectroscopic fluorescence detection approach is presently able to detect NADH concentrations of 0.025% (350  $\mu\text{M}$ ).

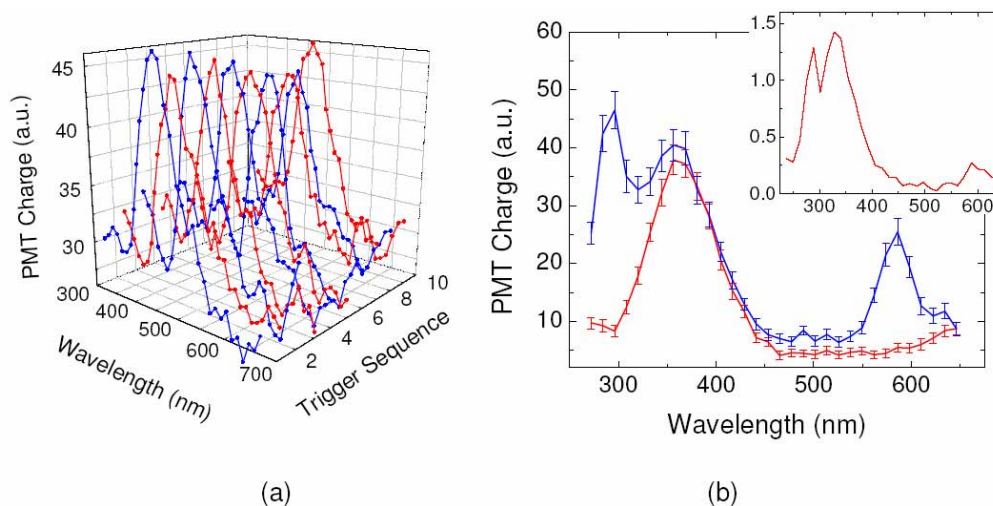


Fig. 4. Single particle fluorescence spectra. (a) Ten sequential 0.025% NADH-doped water droplets under 340 nm excitation. (b) 290 nm excitation of single 0.5% tryptophan-doped water droplets with (lower curve) and without (upper curve) an additional LED-scatter blocking filter. Inset shows average over 500 particles of 6  $\mu\text{m}$  diameter dry tryptophan.

Employing a 290 nm UV LED array, we acquired spectra from a single 0.5% tryptophan-doped water droplets as shown in Figure 4(b). The upper trace, with a visible second-order peak from the diffraction grating arising from elastically scattered light, was acquired without the additional LED-scatter blocking filter. This illustrates the necessity for the supplemental filter, and shows that the fluorescence lineshape, shown in the lower trace with the filter, is minimally distorted by the chosen emission filters. The error bars show the standard deviation of the signal as measured over 100 nominally identical water droplets. One possible source for the deviation is that not all particles are successfully tracked throughout their entire trajectory, and hence all particles are not equally illuminated. For example, particles may

have slightly different velocities or may be traveling in a trajectory that is at the edge of the 200  $\mu\text{m}$  illumination width, effects that are aggravated by the long particle tracking distance of approximately 3 mm. The spectroscopic optical system under development in our laboratory contains an LED-derived scatter channel for simultaneous fluorescence and elastic scatter collection so that particle size and illumination non-uniformities can be normalized out, as is done in the filter-based system described above. Furthermore, the electronics to handle real-time spectral algorithms on a single particle basis are in development.

### 3.3 Dry particles

In a fieldable bio-aerosol fluorescence detector, dry particles are collected from the ambient and passed through the system as collected. For testing purposes, we generated dry tryptophan particles using the MicroDrop generator with a drying column from an Ink Jet Aerosol Generator (IJAG) system [15] and confined the particle stream with a nozzle. Although the MicroDrop generator produces a single particle per trigger with a constant delay and a narrow jetstream, the inclusion of the drying column and nozzle yields a wider jetstream and particles which arrive at irregular times. In this case, which closely resembles the case of ambient collected particles, the red LD trigger is absolutely required for timing. In this initial work, 0.5% doped water droplets were dried to form 6  $\mu\text{m}$  tryptophan particles and used in the spectroscopic detection system described above. The inset of Fig. 4(b) shows first results from these experiments. By detecting elastic scatter from two red LDs separated by 3 mm along the particle flight path, we measured an average particle velocity of 9 m/sec, yielding an integration time of only 350  $\mu\text{sec}$ . Due in part to the reduction in illumination time, and hence total number of photons delivered to the particle, the real-time single particle spectra from dry particles were rather weak and required further data processing. The spectrum in Fig.4(b) (inset) is averaged over 500 sequential trigger events during which time the 290 nm array was operated at an injection current of approximately 35mA yielding an output power of 60  $\mu\text{W}$  per element. The additional LED-scatter blocking filter is absent in this spectrum, and clear tryptophan and LED-scatter peaks are seen to match the water-doped tryptophan data shown in the same figure. A more complete characterization of the performance of our spectroscopic system using dry particles will be presented elsewhere.

## 4. Conclusion

These demonstrations of application and utility of linear arrays of UV LEDs in a fluorescence-based bio-aerosol detection system illustrate the emerging capability of UV LEDs, in conjunction with novel detector arrangements, to shrink the size and cost of systems currently employing solid-state lasers. While there is room and need for significant improvement in the UV LED efficiency, the use of both 340 nm and 290 nm LEDs, featuring a flexible LED array design and a smaller detector configuration, reflects the maturation of the concepts behind a next generation of compact biowarning systems which access key biological fluorophores such as NADH and tryptophan. Our LED array-based instrument collects full real-time spectroscopic data, which allows for the implementation of further discrimination routines, and thus offers a real alternative to the earlier generation of large and expensive laser-based systems.

## Acknowledgments

We gratefully acknowledge the contributions by Ling Zhou, W. Goetz, and M. Krames of Lumileds LLC to this work, which is supported by the Defence Advanced Research Projects Agency SUVOS program under SPAWAR Systems Center Contract No. N66001-02-C-8017